Earth Surface Processes and Landforms
Earth Surf. Process. Landforms **33**, 1977–1992 (2008)
Published online 13 May 2008 in Wiley InterScience
(www.interscience.wiley.com) **DOI:** 10.1002/esp.1649

Temporal changes in suspended sediment transport in a gullied loess basin: the lower Chabagou Creek on the Loess Plateau in China

H. Y. Fang,[1,2] Q. G. Cai,[1]* H. Chen[1] and Q. Y. Li[3]
[1] *Key Laboratory of Water Cycle and Related Land Surface Processes, Institute of Geographic Sciences and Natural Resources Research, Chinese Academy of Sciences, Beijing, China*
[2] *Graduate School of Chinese Academy of Sciences, Beijing, China*
[3] *Yantai Institute of Coastal Zone Research for Sustainable Development, Chinese Academy of Sciences, Yantai, China*

**Correspondence to: A11 Datun Road, Anwai, Chaoyang District, Beijing 100101, China.*
E-mail: caiqg@igsnrr.ac.cn

Received 9 April 2007;
Revised 5 November 2007;
Accepted 19 November 2007

Abstract

Suspended sediment dynamics are still imperfectly understood, especially in the loess hilly region on the Loess Plateau, with strong temporal variability, where few studies heretofore have been conducted. Using a dataset up to eight years long in the Lower Chabagou Creek, the variability in suspended sediment load at different temporal scales (within-flood variability, monthly–seasonal and annual) is analyzed in this paper. The results show that, on the within-flood scale, most of the sediment peaks lag behind peak discharges, implying that slope zones are the main sediment source area; independent of the occurring sequences of the peaks of sediment and discharge, all the events could present an anti-clockwise hysteresis loop resulting from the abundant material and the influence of hyperconcentrated flows on suspended sediment concentration. At monthly and seasonal scales, there is a 'store–release' process, i.e. sediment is prepared in winter, spring and late autumn, and exported in summer and early autumn. At the annual scale, the high variability in concentration and sediment yield are highly correlated with water yield, resulting from the number and magnitude of floods recorded yearly, and almost all the suspended load is transported during these events.

Keywords: sediment peak; peak discharge; hysteresis loop; hyperconcentrated flow; Chabagou Creek

Introduction

Over recent decades, interest in suspended sediment dynamics has increased, and many issues such as the transport of the pollutants adsorbed onto the fluvial sediments, reservoir sedimentation, channel and harbor silting, soil erosion and loss, as well as the ecological and recreational impacts of sediment management, relate to suspended sediment concentration, implying the requirement to understand its occurrence and transport process (Ferguson, 1986; Novotny and Chesters, 1989; Walling *et al.*, 1999; Horowitz *et al.*, 2001; Gardner and Kjerfve, 2006). Furthermore, study on suspended sediment concentration can provide important information on processes of erosion and deposition as well as different erosion sources within basins, such as hillslope erosion and channel erosion, runoff from agricultural land, construction activities and sewage, and industrial effluents (e.g. Collins *et al.*, 1997; Rondeau *et al.*, 2000). Thus, more and more work on suspended sediment dynamics in temporal scales have been conducted in many regions around the world, such as in Spain (e.g. Rovira and Batalla, 2006), Italy (e.g. Lenzi and Marchi, 2000), Germany (Wood, 1977; Spott and Guhr, 1994; Asselman, 1999), the UK (e.g. Walling and Webb, 1982; Haifa, 1984; Williams, 1989), the USA (e.g. Gomez *et al.*, 1997; Magilligan *et al.*, 1998), Mexico (Hudson, 2003), Israel (Alexandrov *et al.*, 2003), Japan (Siakeu *et al.*, 2004) and China (Chen *et al.*, 2006). However, few studies of suspended sediment transport have been conducted in Yellow River drainage basins under strong contrast and, especially, in deeply and densely dissected loess hilly areas on the Loess Plateau, where suspended sediment concentration in runoff is among the highest on

Earth, resulting from the easy erodibility of loess soil, harsh climatic conditions and low vegetation coverage. The aim of this study is to analyze the dynamics of the suspended sediment transport at different temporal scales (within floods, between months and seasons and between years) in the Chabagou Creek, a representative example of the fluvial dynamics and water and sediment uses in loess hilly region on the Loess Plateau of China.

Material and Methods

Study basin

The research is conducted in the Chabagou basin (Figure 1), located in the loess hilly region on the Loess Plateau. The Chabagou basin covers an area of 205 km^2 (109°47′ E and 37°31′ N, 900–1100 m a.s.l.), with mean basin length 26·30 km and width 7·76 km. The mean gradient of the whole basin is 522‰. The climatic is semi-arid with mean annual precipitation 450 mm, varying from 300 to 600 mm in the drainage basin, around 70% of which predominantly falls from June to September, usually falling as high-intensity and short-duration rainstorms. The river system within the basin comprises the main river Chabagou Creek (24·1 km long) and its 11 tributaries, four of which are located on its right and seven on its left. The Chabagou Creek is a permanent river; however, most of the water flows and sediments occur in the flood season. The natural vegetation was totally destroyed several hundred years ago and hillslopes are cultivated as farmland. The Chabagou basin possesses Malan loess with less than 40% clay particles, leading to its large porosity and easy erodibility (Kimura *et al.*, 2005). The mean annual sediment yield is 15 780 t km^{-2} $year^{-1}$, ranging from 6267 to 23 670 t km^{-2} $year^{-1}$.

Data source, treatment and measuring station

To collect data for the purposes of engineering design and scientific research in respect of soil and water loss on the Loess Plateau, a dense network of hydrometric stations was established by the Yellow River Commission from the 1950s, where water discharge and suspended sediment concentration were measured regularly. As most of the flood events last for just a short period of time, the events were intensively sampled, and the sampling interval was generally less than 10 min. The water level was observed at a staff gauge or flume, and flow discharge was obtained using previously established discharge–water level curves. The curves were calibrated according to measurements of flow

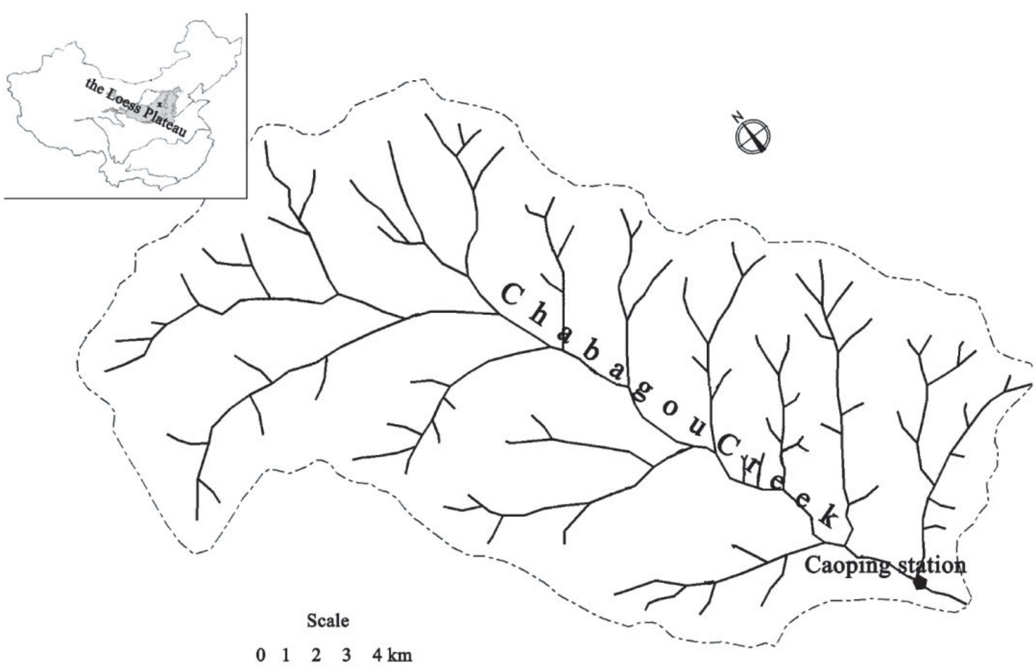

Figure 1. Location map of the Chabagou Creek.

DOI: 10.1002/esp

discharge obtained using current meters. Samples of water and suspended sediment were taken using horizontal samplers or bottles, and the sediment samples were analyzed in the laboratory to determine sediment concentration, which was used as a surrogate for the cross-section concentration; this approach was used because of the approximately uniform distribution of sediment concentration throughout the cross section. Based on the results of water discharge, time interval and suspended sediment concentration, sediment load or sediment yield can be calculated for each time interval of the event. Then event-averaged sediment concentration was calculated by the event sediment yield divided by the event volume of runoff. The same method was used to calculate monthly and yearly sediment concentrations through dividing the total sediment by the total runoff for each time period. At almost all the hydrometric stations, self-recording hyetographs and/or common hyetographs were installed, thus the rainfall characteristics were obtained.

All the measurements of rainfall characteristics, water stage, discharge, suspended sediment concentration and suspended sediment load at all stations follow national standards issued by the Ministry of Water Conservancy and Electric Power (e.g. 1962, 1975), and were printed for internal use. The procedures used for hydrological survey, sampling and laboratory analyses at hydrometric stations in China are basically the same as used internationally. For a detailed introduction, please also see the work of Yan (1984).

The study was carried out at the Caoping hydrologic station, one of the stations mentioned above, located in the loess hilly region on the Loess Plateau lying downstream in Chabagou Creek (Figure 1), 1·3 km away from river mouth. The area controlled by Caoping station is 187 km^2. At the Caoping hydrologic station, the riverbed is composed mainly of bedrock without sediment siltation, and the mean channel slope is estimated to be 8‰. The station was established by the Yellow River Commission of Water Conservancy in 1959, and closed in 1969, thus 11 years (1959–1969) of data are available. However, for integrity of the recorded data, the dataset in the time period 1960–1967 were selected in the present study at the Caoping hydrologic station.

Results

Within-event sediment variability

Although many studies of suspended sediment concentration–discharge relations for individual events have been conducted, because of differences among study regions there is only a partial understanding of the internal dynamics (e.g. Williams, 1989; Mossa, 1988; Sichingabula, 1998; Rovira and Batalla, 2006). The concentrations of all sediment samples collected during 1964, exemplified here, are plotted against discharges in Figure 2, demonstrating that there is

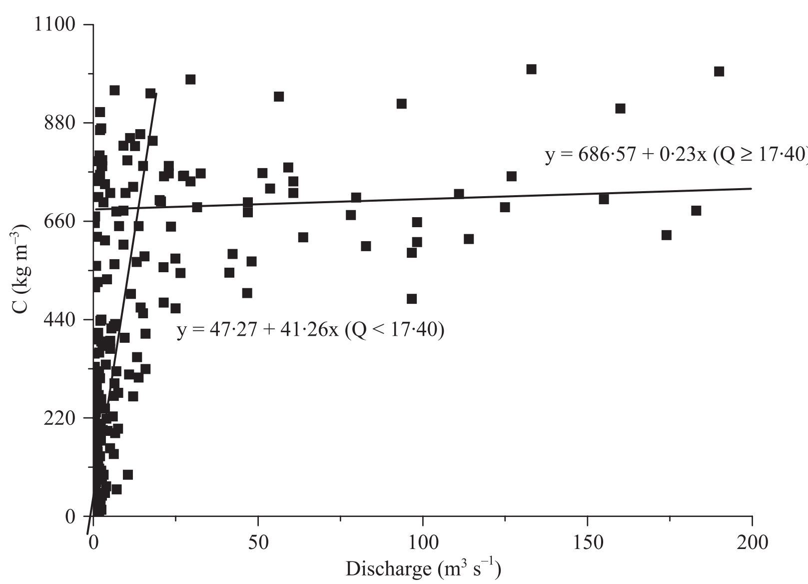

Figure 2. Relationship between suspended sediment concentrations (*C*) and water discharges exemplified by the floods that happened in 1964.

DOI: 10.1002/esp

a high amplitude of concentration, especially within the lower discharge range. However, when water discharge (Q) is larger than a certain value, 17·0 m^3 s^{-1}, the scatter of suspended sediment concentration (C) with water discharge becomes small. The suspended sediment concentration is influenced by complicated factors, including sediment availability, its occurring time, the physical properties of the sediment particles, flow discharge, especially its fluid mechanism and others (see, e.g., Walling *et al.*, 1979; Haifa, 1984; Gong and Jiang, 1978; Gong and Xiong, 1980; Wang *et al.*, 1982; Chen, 1983; Steegen *et al.*, 2001; Steegen and Govers, 2001; Hudson, 2003). Abundant loose material often exists prior to rainstorms after hoeing for the cultivated lands, which leads to less energy expenditure for stream flow, and hence a higher C value occurs; otherwise, more energy will be required to detach soils and a lower value of C is expected. Consequently, even for the same flow event, especially for the smaller ones, differences in land surface condition will result in a variation in suspended sediment concentration. Lower water discharges usually result from lower rainfall intensity. For these events, most of the water discharge may be lower than the critical value (i.e. 17·0 m^3 s^{-1}), the eroded sediment is characterized by fine particles and the median grain size of sediment increases with increasing rainfall intensity (Wang *et al.*, 1982), implying considerable variation in the particle size of the fluvial sediment. Generally speaking, higher water discharge corresponds to higher sediment concentration; however, for lower water discharge, other factors, such as land surface condition, channel slope and cross-section shape, intensively influence sediment yield, leading to a larger difference in C values. More importantly, the flow mechanism for lower water discharges can lead to considerably larger difference in suspended sediment concentration, which will be discussed in the following sections. All the factors give an over 800-fold range of the C values at lower flows. However, for the water discharge exceeding the critical value 17·0 m^3 s^{-1}, the less scattered C values with discharge can be attributed to the reducing functions of the other factors in influencing sediment yield compared with the water discharge. In other semiarid regions, less varying C values for larger discharges have been verified, as in the extensive badland along the Red Deer River in the semi-arid prairie region of southern Alberta, Canada, by de Boer and Campbell (1989) and in the Eshtemoa region lying 18 km northeast of Beer Sheva by Alexandrov *et al.* (2007). Particularly interesting is that more scattered C values for the lower discharges and less scattered C values for the larger ones, averaging 686 kg m^{-3} in value, in Chabagou basin can be predicted by two rating curves with respect to water discharge with two different slopes (Figure 2). We notice that the slope for the discharges larger than 17·0 approaches zero, implying that the mean C has little change when the discharge is larger than the critical value. This C–Q relation is slightly different from those in other regions, such as in the upper part of the River Rother of West Sussex, a major tributary of the River Arun with an area of 153·9 km^2 (Wood, 1977), in the Cordon Watershed in the Eastern Italian Alps (Lenzi and March, 2000) and in the northern part of the Catalan Coastal Ranges, 60 km northeast of Barcelona (Rovira and Batalla, 2006), where the slopes of the C–Q lines are still larger even when discharges are larger.

As in the studies by others (e.g. Williams, 1989; Alexandrov *et al.*, 2007), the scattered C–Q relation often show a hysteretic behavior related to a lag time between peaks of water and sediment. According to the occurring sequences of the peaks of sediment and discharge, the floods in Table I can be grouped into three types for the 49 recorded events during the period 1960–1967. Type I indicates the floods during which the sediment peaks lag behind the peak discharges; type II is for the floods that have a good time agreement between sediment peaks and peak discharges and type III is the floods of which the sediment peaks precede the peak discharges. Table I shows that there are 31 type I floods, occupying 63·2% of the total, and nine floods for both types II and III, each occupying 18·4%. With respect to the sediment concentrations for the recorded events in Table I, the mean maximum sediment concentration is 796·5 kg m^{-3}. For type I flood events, the mean sediment concentration is 599 kg m^{-3} when the maximum discharge approaches, which is less than 25% of the mean maximum sediment concentration. Type III flood events, corresponding to the maximum discharge, have a mean sediment concentration 783 kg m^{-3}, less than 10·8% of the averaged maximum sediment concentration. The mean sediment concentration is 701 kg m^{-3} for type II events. This phenomenon could be attributed to the condition of available material and flow mechanism during its duration.

Williams (1989) pointed out that the C/Q ratio is an index in determining C–Q relations. Though the occurring sequences of peaks of water and sediment are different (Table I), the resulting C–Q relations follow an anti-clockwise behavior (Figure 3), resulting from the higher suspended sediment concentration on the Q-graph falling limb for a given Q value. For instance, the C_1/Q_1 and C_2/Q_1 ratios for the flood on 21/5/67, which is a type I flood, were 4 and 47 respectively, with $Q_1 = 20$ m^3 s^{-1}. For the type II flood on 3/6/63 the C_1/Q_1 and C_2/Q_1 ratios for a given discharge $Q_1 = 23$ m^3 s^{-1} were 16 on the rising limb and 35 on the falling limb, and for the type III flood on 28–30/8/63 the C_1/Q_1 and C_2/Q_1 ratios were 30 on the rising limb and 62 on the falling limb for a given discharge $Q_1 = 13·5$ m^3 s^{-1}. Hence, due to the continuous higher concentration value independent of the smaller discharge on the C-graph (the concentration–time-graph) falling limb, the higher C/Q ratio on the Q-graph (the discharge–time-graph) falling limb compared with that on the Q-graph rising limb for the same value of Q induces an anti-clockwise loop (Figure 3),

DOI: 10.1002/esp

Table I. Flood events during the period 1960–1967 at the Caoping hydrometric station

	Q_p ($m^3 s^{-1}$)			C_p ($kg m^{-3}$)						
Day	Time (h:m)	Q	C	Time (h:m)	Q	C	Water yield ($10^3 m^3$)	Sediment yield (10^3 t)	Duration (h)	Type
24–25/6/60	17:42(24)	6·23	482	18:16(24)	3·1	620	37·872	15·218	31	I
2–3/7/60	17:26(2)	84·5	693	17:33(2)	77·3	923	364·534	294·764	16	I
5–6/7/60	17:36(5)	31·2	847	17:50(5)	22·9	899	248·342	191·518	15	I
11–12/7/60	18:36(11)	19·5	794	18:36(11)	19·5	794	71·579	38·489	30	II
19–20/7/60	18:23(19)	63·8	849	18:20(19)	14·9	893	279·437	192·467	14	III
27–28/7/60	21:00(27)	18·5	594	21:00(27)	18·5	594	130·26	54·510	30	II
31/7–1/8/60	21:22(31/7)	113	606	21:28(31/7)	105	787	429·964	316·583	15	I
3/8/60	7:45(3)	3·55	139	9:00(3)	1·5	435	30·109	4·749	17	I
10–11/8/60	19:20(10)	55·0	505	19:20(10)	55·0	505	445·934	157·530	19	II
24–25/9/60	6:40(24)	129	542	15:00(24)	16·4	601	1616·038	801·643	36	I
26–27/9/60	23:00(26)	10·5	307	23:00(26)	10·5	307	132·006	26·089	28	II
21–23/7/61	7:20(21)	172	883	8:45(21)	18·4	915	1035·782	761·237	66	I
30/7–2/8/61	19:02(30/7)	654	853	18:50(30/7)	254	914	2557·181	1835·460	55	III
13/8/61	13:00(13)	75·1	440	14:00(13)	26·8	594	807·236	293·259	22	I
16/8/61	1:21(16)	89·7	864	1:21(16)	89·7	864	412·437	292·195	22	II
26–27/8/61	10:20(26)	5·27	146	13:00(26)	0·815	590	82·847	12·294	27	I
26–28/9/61	4:45(27)	116	125	5:30(27)	35·6	777	1373·242	558·957	51	I
27–28/6/62	13:37(27)	12·6	7·15	13:40(27)	12·6	787	51·236	17·612	29	I
23–24/7/62	7:42(23)	44·7	945	9:00(23)	26·3	979	361·726	282·451	36	I
1–3/8/62	18:15(1)	37	685	18:24(1)	37	797	250·244	142·017	47	I
11–13/8/62	24:00(11)	118	823	0:35(12)	37·2	835	549·834	385·327	42	I
22–24/5/63	11:42(23)	83	845	12:00(23)	58·0	1020	596·573	406·516	32	I
3–4/6/63	17:22(3)	131·0	1010	17:22(3)	131·0	1010	452·362	414·841	15	II
15–16/6/63	22:34(15)	10·8	417	22:00(15)	10·2	537	95·213	30·615	15	III
29/6/63	22:00(29)	3·1	116	22:30	2·7	740	25·526	12·734	10	I
6–7/7/63	6:18(6)	27·7	401	7:00(6)	15·8	653	260·352	109·820	24	I
26–27/8/63	20:36(26)	585·0	1020	20:32(26)	554·0	1220	1885·627	1830·758	22	III
28–29/8/63	21:56(28)	187·0	707	20:00(28)	6·8	855	776·853	564·206	17	III
29–30/4/64	19:42(29)	190·0	953	19:51(29)	133·0	1000	536·630	473·818	29	I
5–6/7/64	1:24(6)	183·0	684	2:00(6)	127·0	760	1337·242	1057·786	41	I
14–17/7/64	0:15(15)	79·8	713	18:43(16)	14·3	855	674·266	415·083	62	I
2/8/64	15:26(2)	155·0	709	16:30(2)	27·6	762	603·542	409·268	13	I
23–24/8/64	23:12(23)	6·3	139	24:00(23)	2·4	391	47·722	26·248	28	I
11–12/9/64	0:30(12)	96·7	589	0:30(12)	96·7	589	545·834	242·174	28	II
17/9/64	3:30(17)	31·5	691	5:00(17)	9·2	829	238·276	158·471	24	I
1–2/8/65	22:21(1)	65·7	794	22:26(1)	63·5	1030	263·374	178·842	8	I
4–6/8/65	15:54(4)	23·6	504	16:22(4)	15·0	678	296·352	148·294	36	I
9–10/8/65	3:12(9)	26·8	848	3:12(9)	26·8	848	115·344	51·302	24	II
26–28/6/66	15:51(27)	225	753	17:48(26)	167	921	2739·744	2046·470	51	III
17–19/7/66	19:24(17)	993	809	5:02(18)	8·32	947	6746·754	5230·510	39	I
9–10/8/66	18:26(9)	81·2	870	18:14(9)	58·7	932	446·688	357·862	17	III
15–16/8/66	19:57(15)	1520	705	1:05(16)	6·67	975	5327·424	4135·856	30	I
28–29/8/66	20:00(28)	581	755	20:06(28)	496	804	1617·408	1203·670	16	I
21–22/5/67	18:25(21)	53·5	870	20:00(21)	17·6	1020	336·096	266·386	36	I
17–18/7/67	17:37(17)	167·0	876	17:22(17)	161·0	887	1009·152	790·251	28	III
22–23/8/67	4:06(22)	60·8	702	3:54(22)	56·5	745	664·416	363·378	41	III
26–27/8/67	16:14(26)	289·0	803	16:16(26)	276·0	820	1595·808	1190·759	30	I
1–2/9/67	0:15(1)	114·0	802	0:15(1)	114·0	802	698·112	59·762	32	II
13–15/9/67	19:42(13)	38·8	715	20:15(13)	21·2	988	419·904	91·871	52	I

The figures in the parentheses represent the day when peak discharge (Q_p) and sediment peak (C_p) happen; I indicates the floods within which the sediment peaks lag behind the peak discharges, II indicates the floods that have a good time agreement between sediment peaks and peak discharges and III indicates the floods within which sediment peaks precede peak discharges.

DOI: 10.1002/esp

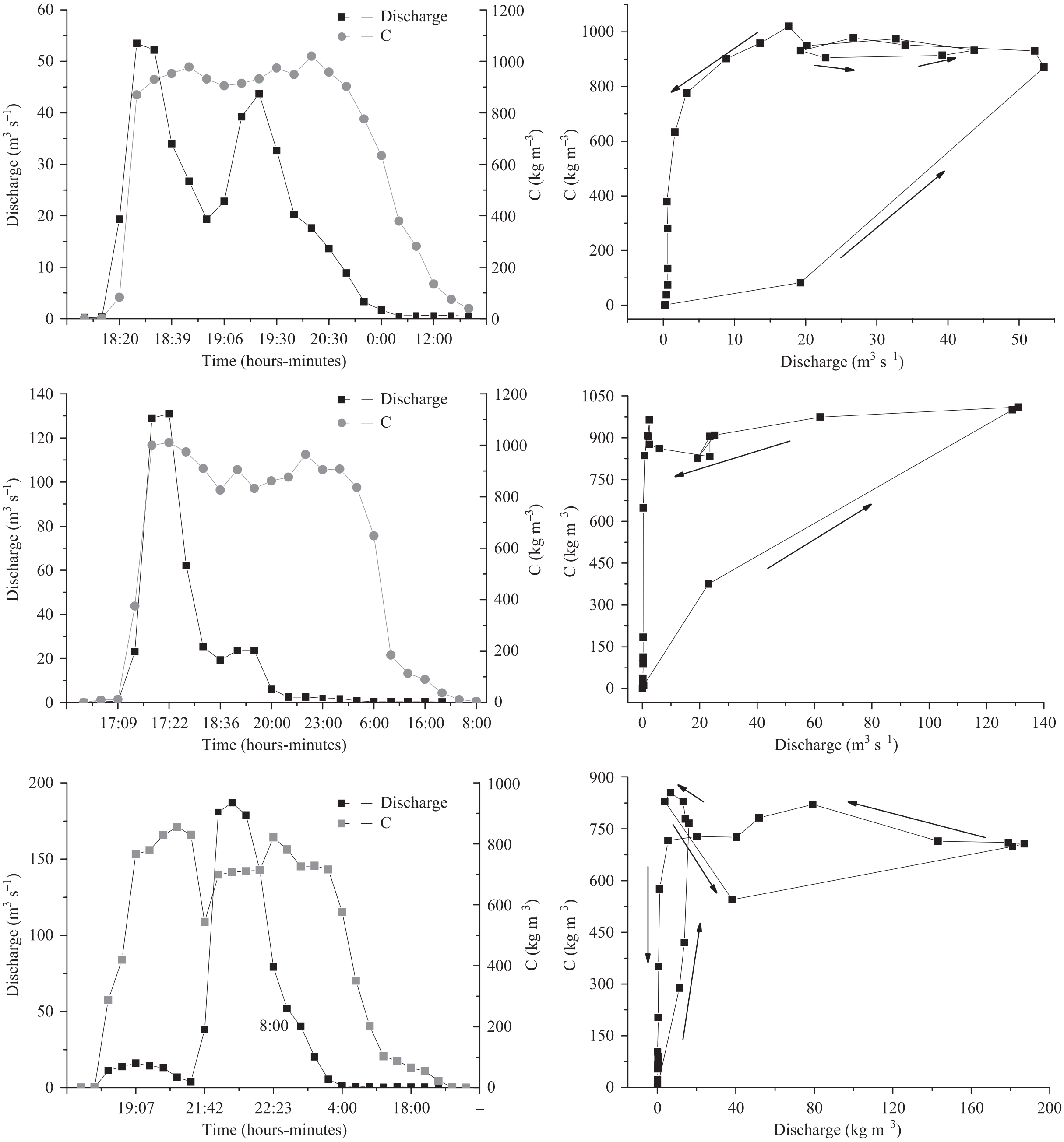

Figure 3. Three types of relation of discharges versus suspended sediment concentrations (*C*): Type I, the *C* peak lags behind that of discharge, exemplified by the flood on 21/5/67; type II, the *C* peak has a time agreement with peak discharge exemplified by the flood on 3/6/63, and type III, the *C* peak precedes that of discharge, exemplified by the flood on 28–30/8/63.

belonging to Williams' (1989) class III response for type I and type II floods, while exemplified type III event is a new type of event that Williams (1989) did not mention, resulting from the special erosion environment in the study area. It should be noticed that for some other type III events the second sediment peak probably does not occur, and their C–Q relations for them still belong to Williams' (1989) class III response.

Samples in Figure 3 show that the durations of concentrations on Q-graph falling limbs were 3 and 30 times of those on the Q-graph rising limbs for type I and type II floods, and as for the type III flood, though the sediment

DOI: 10.1002/esp

peak precedes the peak discharge by almost 2 hours, the duration of concentration on the Q-graph falling limb was still 1·9 times that on the Q-graph rising limb. When the integrals of the sediment transported over the events are computed, on the Q-graph falling limbs the exported suspended sediment loads occupied 95% of the total for the flood on 21/5/67, 83% for the flood on 3/6/63 and 81% for the flood on 28–30/8/63. They could be attributed to the sediment sources and flow mechanism of the transporting sediment. The higher concentration in conjunction with its longer duration in the Q-graph falling time makes an intensive transportation capacity of the flow.

Monthly and seasonal variability

The mean C values range from 0·037 kg m^{-3} in January to 497·373 kg m^{-3} in August. Based on the mean monthly values of C and Q, most of the C–Q relations produce clockwise loops (Figure 4), different from those of the flood events in Figure 3. Exceptionally, monthly C–Q relations in 1964 and even 1965 present anti-clockwise loops, which may be caused by abruptly occurring or increased gravitational erosion, human activities or other factors inducing an abnormal phenomenon (e.g. higher C values occur for lower Q values in April 1964), but they do not disrupt their seasonally changing trend. Seasonally, all the C values tend to be higher in summer (from June to August) and early autumn (i.e. September) than winter, spring and late autumn (November and December) (Figure 4). On the Loess Plateau, most of the rainfalls as well as runoffs occur from June to September, and the suspended sediment concentrations during this period are much higher than those in other months. For example, the maximum sediment concentration in August 1963 is up to 850 kg m^{-3}, while the minimum in January almost zero (0·045 kg m^{-3}). On average, the monthly sediment concentrations are 187 kg m^{-3} in June, 471 kg m^{-3} in July, 483 kg m^{-3} in August and 174 kg m^{-3} in September, whereas in other months the sediment concentration is not more than 100 kg m^{-3}, and even approaches zero from November to March. The condition of monthly concentration distribution leads to broad proportionality of the hysteresis loops between discharge and sediment concentration (Figure 4). Furthermore, for higher correlation between monthly water and sediment yields ($r = 0{\cdot}970$), most of the sediment loads are produced for these months, and the suspended sediment yields in other months are very much lower (Figure 5). On average, more than 95% of the total annual suspended sediment load is transported during the summer (from June to August) and early autumn (i.e. September), the period in which the largest number and amplitude of floods and the maximum water yield (65% of the annual total) occur. However, the total suspended load transported during winter (December to February) occupies less than 0·004% of the annual total, though the water yield is up to 6·8% of the annual water yield in the same time period. The percentages of the total annual suspended load exported in the spring and later autumn seasons are less than 4 and 0·3% respectively (Figure 6). From these results, a 'store–release' process of available sediment can be inferred for sediment transport. During the store phase, sediment is prepared in the basin by weathering, human activities and the erosion process (winter, spring and later autumn), followed by the release phase, in which most of the sediment is transferred downstream in summer and late autumn. Hyperconcentrated flow, frequently happening in the loess hilly region on the Loess Plateau, is a special 'two-phase solid–liquid flow' (Xu, 1999, 2004), which has an intensive erosion property. During a time period with few or no high-intensity rainstorms, the occurring frequency of hyperconcentrated flows is low, and the material already prepared may be stored on slope surfaces, the channel bank and/or the channel bed (Figure 7). When a high-intensity rainstorm occurs, generally in summer and late autumn, hyperconcentrated flows can frequently occur, and the previously stored material can be released rapidly. Based on different-order basins and/or different events on the Loess Plateau, several workers (Gong and Jiang, 1978; Mou and Meng, 1982; Jing *et al.*, 1993; Cai *et al.*, 1992; Liu *et al.*, 2005) have found that the mean annual sediment delivery ratio was unity, implying that all the 'prepared' materials can be exported by flows through the 'store–release' process.

Annual suspended sediment variability

The variability in concentration and sediment yield accompanied by water yield for the study period demonstrates that the higher the water yields, the higher the C values and the higher the sediment yields were (Figure 8). The mean C values vary from 77 to 605 kg m^{-3}, giving a mean annual value of approximately 305 kg m^{-3}. Total suspended sediment transported during the 1960–1967 period was estimated at 3055×10^4 tonnes, averaging approximately 382×10^4 tonnes year^{-1}. The specific sediment yield for the study period was estimated at $2{\cdot}042 \times 10^4$ t km^{-2} year^{-1}. Annually, the suspended sediment load was estimated at 214×10^4 tonnes in 1960, 373×10^4 tonnes in 1961, 86×10^4 tonnes in 1962, 340×10^4 tonnes in 1963, 288×10^4 tonnes in 1964, and 39×10^4 tonnes, 1326×10^4 tonnes and 390×10^4 tonnes in years 1965, 1966 and 1967, respectively. The high degree of variability in suspended load and C values can be primarily related to the number and magnitude of the floods (Table I).

DOI: 10.1002/esp

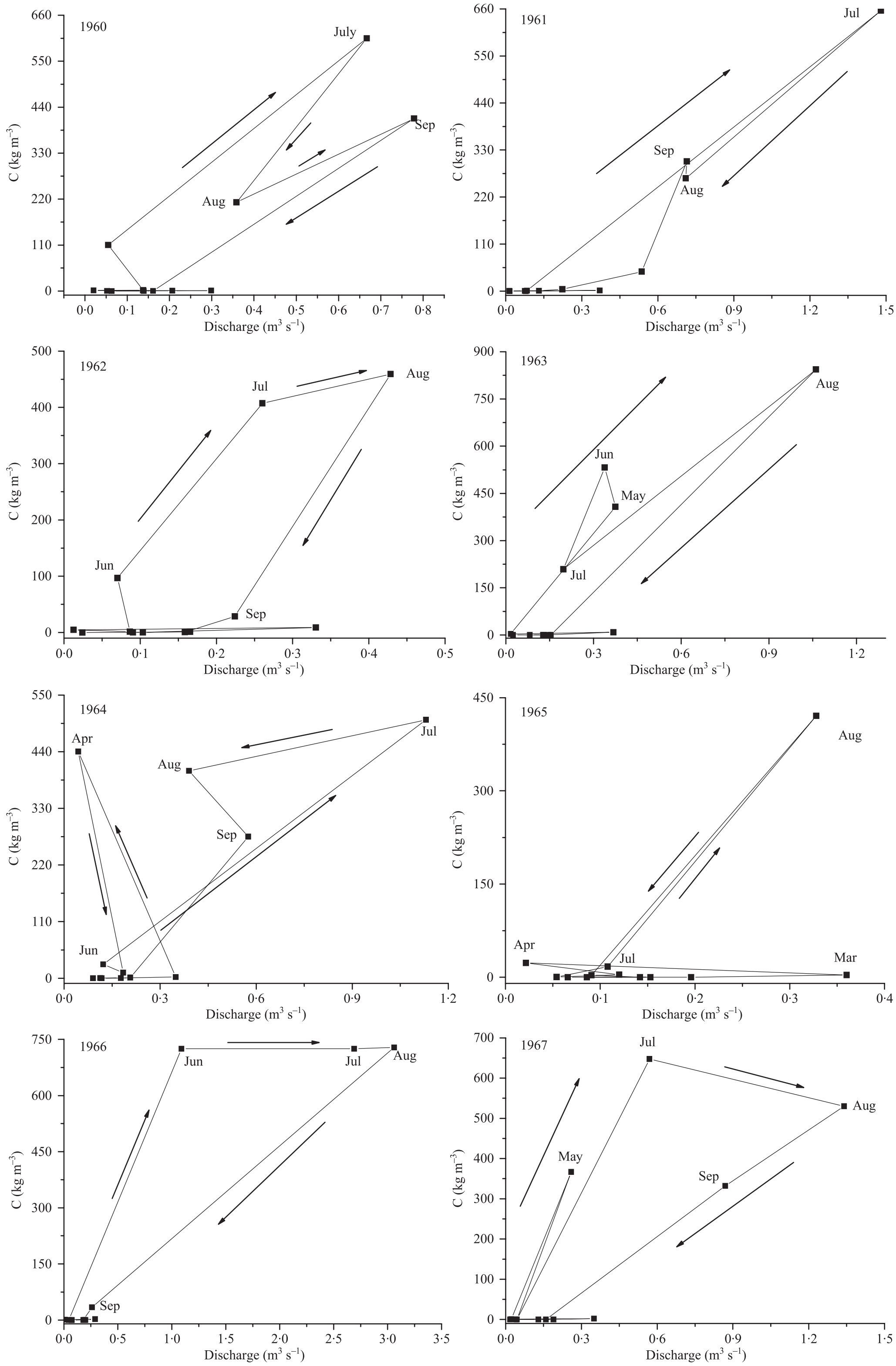

Figure 4. Monthly hysteresis loops of suspended sediment concentration versus discharge during the period 1960–1967 at the Caoping hydrometric station.

DOI: 10.1002/esp

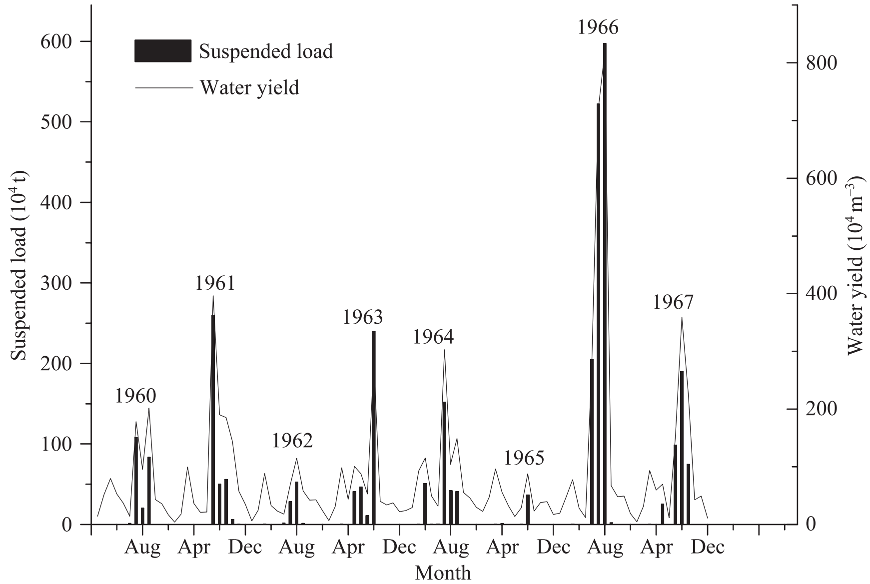

Figure 5. Monthly water yield and sediment load in the Chabagou basin during the study period 1960–1967.

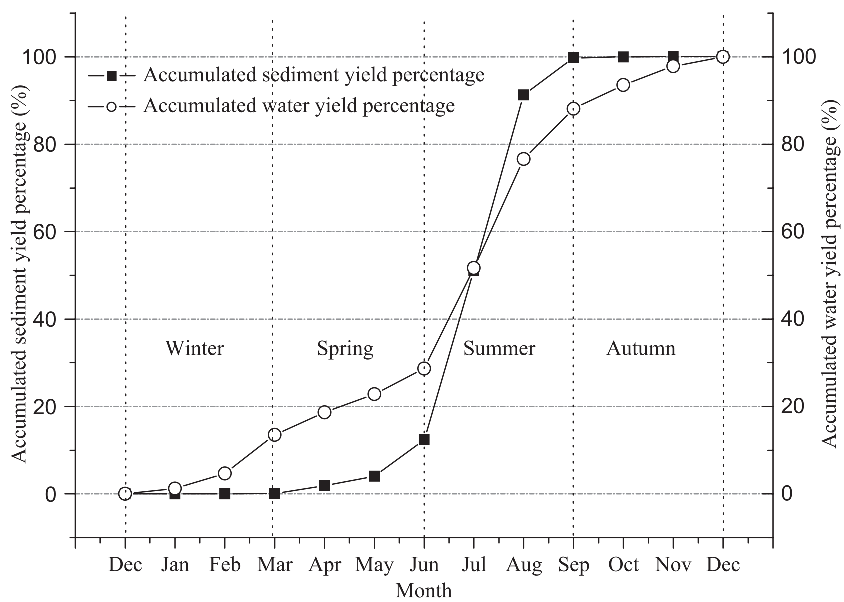

Figure 6. Percentages of the seasonally water yields and sediment loads of the annual mean during the study period.

Discussion

The analysis of the temporal changes in suspended sediment concentration at different temporal scales (within events, monthly and seasonally, and annually) collected in the Chabagou Creek provides insight into the characteristics of the suspended sediment load variability in a gullied loess basin on the Loess Plateau. The suspended sediment concentrations in the study area are exceptionally high. Such high concentrations have not been reported from other loess areas in the world except from some badland areas (see, e.g., Svendsen *et al.*, 2003) and lahars in volcanic regions (see, e.g., Lirer *et al.*, 2001; Lavigne and Suwa, 2004). High sediment concentrations are a characteristic feature of the Loess

DOI: 10.1002/esp

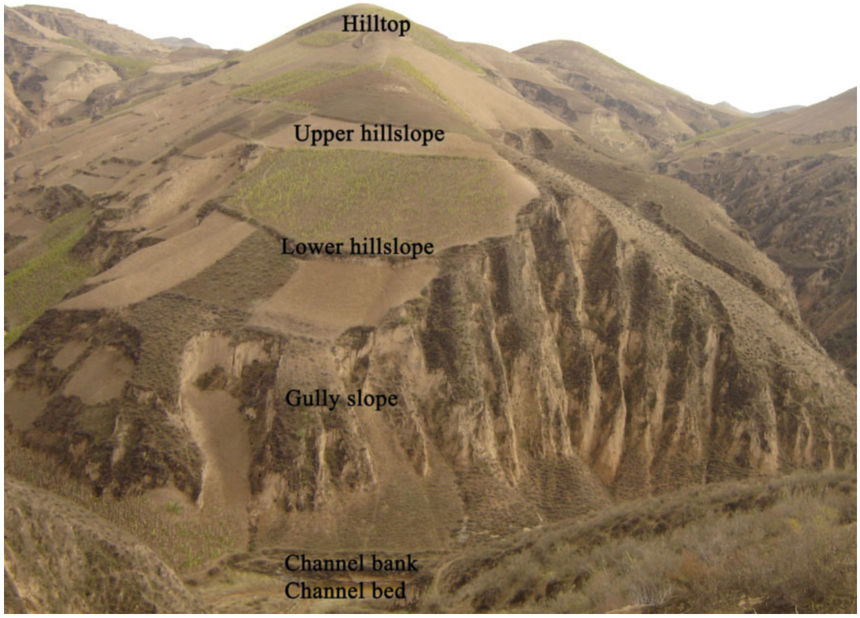

Figure 7. A photograph showing the structure units of the slope–gully system taken in the study region. This figure is available in colour online at www.interscience.wiley.com/journal/espl

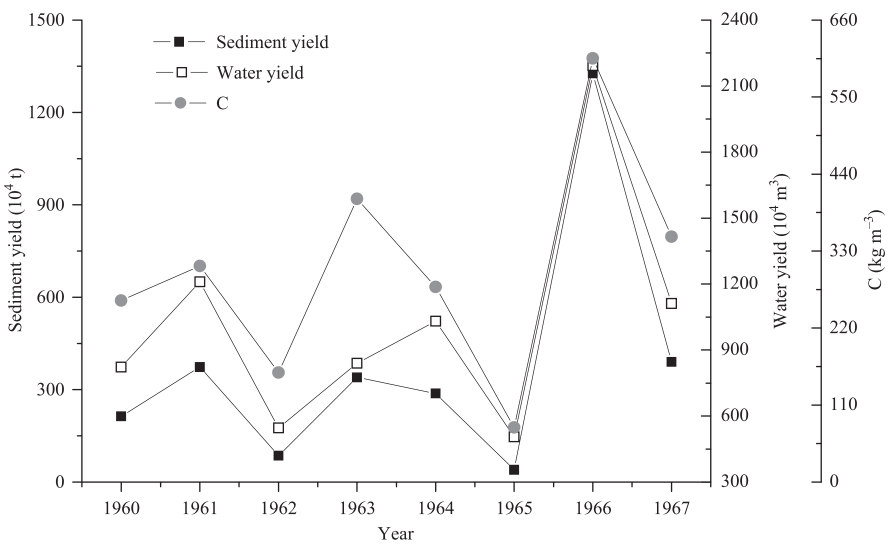

Figure 8. Annual suspended sediment concentration (C) and sediment yield as well as water yield at the Caoping hydrometric station (187 km^2) during the period 1960–1967.

Plateau, which increase with increasing discharges to a certain limit and remain constant after that limit has been reached. In the study area the 'stable concentration' is about 680 kg m^{-3} (Figure 2), which is in accordance with the study by Gong and Jiang (1978) and Wang *et al.* (1982). The high concentrations are probably caused by a combination of factors, in particular the occurrence of erodible materials on slope surfaces and channel bank (Figure 7), the structure and chemical constitution of the loess, and the harsh climate inducing sparse plant cover. The cultivation on slope surfaces is a major factor associated with serious soil and water erosion. With the population increasing, more and more steep land is beginning to be reclaimed. In the study area, 70% of the total arable land is on more than 25°

slopes (Tang *et al.*, 1998), inducing a larger possibility for the poorly structured loess soil to be eroded away. In the gully slope zone, where the slope gradient is more than 35° or even up to 50–70° for the cliffs, active gravitational erosion (including landslide, slumping and toppling) often occurs. Furthermore, channel erosion is another source of sediment available. During high-intensity rainstorms, channel erosion, including bank erosion, advancement of the gully head and even downcutting the channel bed by flow, often occurs (Gong and Xiong, 1980). All the erosion forms mentioned above can lead to a large amount of materials being eroded. Due to the semi-arid climate the vegetation cover is sparse; even after a reforestation activity since the 1970s in the study region, the forest coverage is only 10–15%, and grass coverage 10% or so. Dieckmann *et al.* (1989) found that an increase of 30% in the vegetation may cause a 90% reduction in sediment yield. The increased population induces irrational landuse, such as a large amount of reclamation on steeper slopes, overgrazing, mining, road construction and other human activities, which seriously destroys vegetation cover and further increases sediment yield (Shi and Shao, 2000). Other factors mainly include soil type and composition and intensive precipitation. As an eolian deposit, the grain-size composition of loess is dominated by silt fractions, the structure of which easily collapses in water and disperses to particles readily susceptible to water erosion and transport (Gong, 1988). Furthermore, loess has a loose structure with well developed vertical joints. Its shear strength is low; thus, potential planes for slides and slumps form easily, especially in the gully slope zone (Figure 7). Hence, in the loess region, sediment supply is generally abundant and non-limited, and sediment flux is transport limited. Therefore, the high sediment concentration as well as the *C*–*Q* relations could be attributed to the rainfall characteristics of high intensity with short duration in the study region, which will be discussed in the following section.

Anti-clockwise loops apparently are known, from the paper by Heidel (1956). However, few examples seem to have been published for single hydrologic events. Furthermore, this kind of loop seldom occurs within a large basin (Haifa, 1984). However, in our study region, a basin with an area of 187 km^2, all the *C*–*Q* loops can have anti-clockwise hysteresis, resulting from the complicated factors mentioned above as well as the flow mechanism to be discussed as follows.

Most of the sediment flow in the gullied loess region is hyperconcentrated flow, which can be generalized as a turbulent, solid–liquid two-phase non-Newtonian flow (Xu, 1991, 1999). In the study area, when the suspended sediment concentration is over 300 kg m^{-3}, the flow's physical properties and mechanical behavior may be changed, and become Binghamian flow, or hyperconcentrated flow (Xu, 2004). Wan and Shen (1978) found that with an increase in flow strength the suspended sediment concentration increases, but when the suspended sediment concentration enters the range of hyperconcentrated flow the increased flow strength is not necessarily required to match the further increase in suspended sediment concentration; instead, even at a lower level of flow strength the suspended sediment transport equilibrium can also be maintained, implying that lower flow energy still can maintain higher suspended sediment content, and there would be hardly any sedimentation out of the flow. For example, an 8·85 m^3 s^{-1} water discharge can transport 902 kg m^{-3} sediment flow for the event occurring on 21/5/67, so that the high and even unchanged *C* values can be maintained in the interval of water discharge between the first and second peaks. However, when the discharge is small enough, a slight change of external conditions could change its flow mechanism. For example, for the event occurring on 3/6/63, when the water discharge is 0·82 m^3 s^{-1}, the sediment concentration is higher than 800 kg m^{-3}, however, when water discharge decreases to 0·299 m^3 s^{-1}, the value of *C* suddenly plummets to less than 200 kg m^{-3}. As for the exemplified type III event on 28–30/8/63, the lower *C* value between the two sediment peaks could result from the lack of sediment, while, during the following time, the new supply of the sediment gives a similar sedi-graph to those of type I and type II events. It is interesting that the exemplified sedigraphs present a similar trend on their falling limbs (Figure 3), which can also be attributed to the intensive sediment-carrying capability of hyperconcentrated flow of the lower discharges on their falling limbs. Noticeably, there are threshold values of discharges at which water flow changes from hyperconcentrated flow to non-hyperconcentrated flow, and it can be extended that the influencing factors are complicated and different events have their own thresholds, which are beyond our present study and require to be studied further. Therefore, for all events the longer durations of higher concentration on the *Q*-graph falling limb result in an anti-clockwise hysteresis loop in spite of the occurring consequence of the peaks of sediment and discharge (Figure 3).

The hillslope flow velocity is several orders of magnitude lower than that of the channel flow; therefore, when the sediment source area is the channel, good time agreement between sediment peak and peak discharge, as well as the sediment peak preceding peak discharge, occurs. On the other hand, when the sediment source areas are the basin's slope, or in the case of the upper part of a large basin, the center of gravity of the sediment source area is further from the basin outlet than the center of gravity of the water contributing area, and a sediment peak lagging behind peak discharge occurs. In addition, gravitational erosion is an important erosion form in the study area; because penetration of water takes time, slumps and slides usually occur at the recession stage of a flood rather than at the rising stage, and supply to the gully channel. Therefore, the higher percentage of type I floods (occupying 63·2% of the total) can be

DOI: 10.1002/esp

attributed to sediment influx from erosion areas on slope zones (Figure 7), and the good time agreement between water discharge and suspended sediment transport for type II floods (occupying 18·4% of the total) as well as the earlier occurring time of sediment peaks compared to that of peak discharges for type III floods (occupying 18·4% of the total) can be referred to the availability of fine sediment eroded from the slope surfaces and deposited in the channel network and the material directly eroded from the channel bank When intensive hyperconcentrated flows occur, the leftovers in the channel as well as the material on the bank are carried away. The phenomenon has been verified by the studies by Gong and Xiong (1980) and Chen (1983).

Different erosion patterns for the C–Q relationship can coexist in the same flood: in the type III flood event occurred on 28–30/8/63, the water–sediment relationship can be divided into two phases. In the first phase of the flood, a fast-response contribution from sediment stored in the channel network and/or sediment eroded from channel bank induces a first sediment peak, following a lower C value due to temporary lack of sediment in the channel and/or on the bank, and then the sediment flux from inter-gully hillslopes and/or gully slope activated during this long-duration flood at a higher distance from the measuring station gives a second higher sediment peak, implying that both channel erosion and slope erosion happened during the flood duration.

Because of the quick response of the material in the channel network and/or on the banks, probably followed by the material from slope zones, type III events usually have a higher averaged sediment concentration than that of the type I flood events, especially for the sediment concentration corresponding to the maximum discharge, and the C/Q ratios of this type of flood event are 3·5 and 6·2, corresponding to the mean maximum discharges and the mean maximum sediment concentrations, respectively. For the C/Q ratios of type I events, time is needed for the large amount of material entering channels before the maximum discharge; however, after the peak discharge, a small discharge can cope with the maximum sediment concentration, which leads to a larger range of 3·5–14·5 for the C/Q ratios.

The flood events at the Caoping station usually last 1–2 days; the events within 48 hours occupy 88% of the total, and the flood events lasting less than 30 hours 60% of the total. The short duration of the flood events as well as the Q graph can therefore be attributed to rainfall characteristics in the study area. Figure 9(A) displays the precipitation frequency distribution for the 49 runoff-induced rainfall events recorded at the Caoping station in 1960–1967. Rainfall events up to 30 mm represent some 80% of the rainfall recorded at the Caoping station, and 59% of these had rainfall amounts up to 15 mm. Rainfall events up to 40 mm represent 88% of the recorded runoff-induced rainfall events. Figure 9(B) shows the distribution of rainfall intensities (maximum 30 minute rainfall intensity, I_{30}) and duration of individual rainfall at Caoping station in 1960–1967, which characterizes high rainfall intensity and short duration. For the recorded rainfall events, some 61% have I_{30} larger than 10 mm hr^{-1}, and 33% of the rainfalls larger than 20 mm hr^{-1}, with the highest recorded I_{30} larger than 70 mm hr^{-1}, and the recorded instantaneous rainfall intensity is up to 3·5 mm s^{-1} (Xia *et al.*, 2007). The high rainfall intensity makes runoff occur promptly, usually as Hortonian flow, which leads to a 59.4% runoff production of the mean annual total (Figure 6). Furthermore, the rainfall events are usually less than 600 minutes. Therefore, the sudden increase in flow discharge and sediment concentration during a short time period in Figure 3 can be explained by the rainfall regime of a large amount of rainfall with high rainfall intensity during a short time duration.

For partial rainfall distribution within the study region, the small rainfall events in Figure 9(B) at Caoping station can still lead to a larger flood occurring. For example, the I_{30} on 31/7/60 at Caoping station is less than 0·6 mm hr^{-1}, with a total 0·7 mm rainfall amount; however, at Xizhuang station, a hydrometric station located on upstream of Chabagou Creek, the I_{30} is over 39·5 mm hr^{-1}, with 21.5 rainfall amount. The promptly increased discharge gives a quick increment in sediment concentration, entering the range of hyperconcentrated flow (Figure 3). This kind of water flow has intensive sediment-transport capacity, and larger flood events usually yield more sediments, with the correlation coefficient between them in Table I $r = 0·990$ ($P < 0·001$). In the study region, most of the annual precipitation concentrates on several rainfalls in the flood season, indicating that the sediment was usually moved out of the basin during a few floods, especially for the larger ones. For example, the flood event on 17–19/7/66 produces 523×10^4 tonnes of sediment, which occupied 39·4% of the total in 1966, and the sediment yield for the floods occurring on 26–28/6/66, 17–19/7/66, 15–16/8/66 and 28–29/8/66 was over 95% of the total in 1966. Table I shows that the majority of sediment is moved out of the basin during events in which C reaches 800 kg m^{-3} and discharge is maintained above 10–20 m^3 s^{-1} for a sustained period. The exemplified scattered C–Q relation in Figure 2 demonstrates that when discharge is larger than 17·0 m^3 s^{-1} concentration changes little, and, even independent of water discharge, a longer duration of discharge can yield a large amount of sediment. These indicate that several larger floods in the flood season control the sediment yield.

In the literature found on Northern Shannxi on the Loess Plateau, channels in basins are essentially sediment transporting pathways under natural conditions, and in a time-averaged sense all the eroded materials can be carried away in the floods, mainly due to intensive hyperconcentrated flow erosion (Gong and Jiang, 1978; Mou and Meng, 1982; Tang, 1991; Jing *et al.*, 1993; Cai *et al.*, 1992; Xu, 1999). Then the large amount of material during the floods

DOI: 10.1002/esp

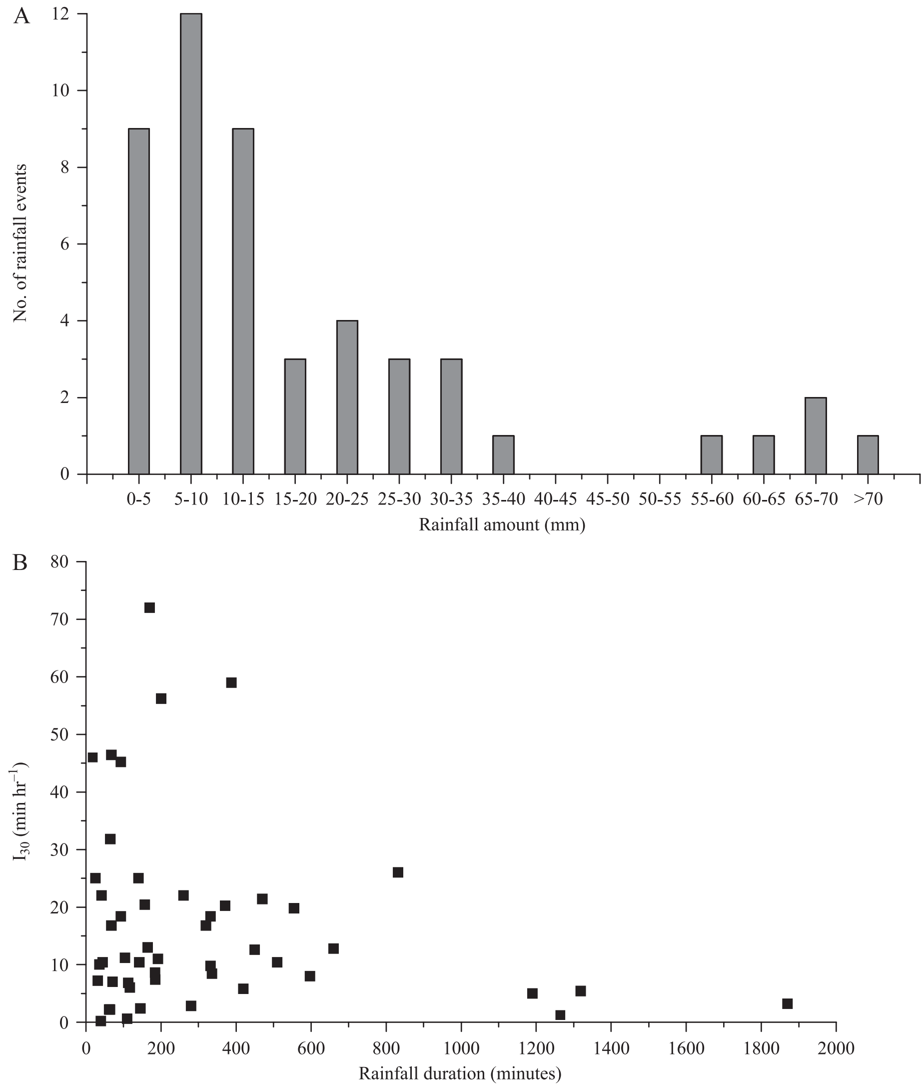

Figure 9. Rainfall characteristics at the Caoping station in 1960–1967: (A) frequency distribution of rainfall amount; (B) relationship between rainfall duration and the maximum 30 minute rainfall intensity (I_{30}).

in Table I, mainly occurring in summer and early autumn, could come from the winter, spring and late autumn, which can be evidenced by the generally occurring clockwise hysteresis loop (Figure 4). During the period of seasons with few rainstorms (i.e. winter, spring and late autumn), the loose loess materials caused by freezing and thawing, human activities and erosion process could not be exported, and probably stay on the slope surface, gully slopes and even channels. During summer and early autumn (i.e. September), the prepared material could be entrained in the flows and exported from the basin, leading to a clockwise hysteresis loop in respect of monthly and seasonal scales. In light of these results, the existence of a seasonal sediment yield cycle composed of two phases of sediment store (winter, spring and late autumn) and release (summer and early autumn) can be defined.

Small spring floods, such as those recorded on 22–28/5/63, 29–30/4/64 and 21–22/5/67, may disrupt this general pattern, in particular, the high suspended sediment concentration recorded in May supports this observation. This kind of sediment 'store–release' process has been verified in the Rhine River (Asselman, 1999) and the Panuco River region (Hudson, 2003). On the Loess Plateau, Xu (1999) explained the 'store–release' pattern through the coupling action of transportation of the hyperconcentrated flows and gravitational erosion.

DOI: 10.1002/esp

Conclusions

This paper describes the variability of suspended sediment transported in the Lower Chabagou Creek at different temporal scales. The variability for different temporal scales presents different erosion–transport patterns. Within the flood scale, according to the occurring sequence of the peaks of sediment and discharge, three types of *C*–*Q* relation were obtained. The largest percentage of type I flood events(occupying 62·3% of the total) indicates that most of the materials directly come from slope zones, and other materials transported in the floods of types II and III are from channel bank and/or the deposited sediment in channel beds. Therefore, the quick response of the material with respect to discharge usually makes type III events of higher concentration than type I events, while they usually have a lower *C*/*Q* ratio range than the type I events. Independent of the occurring sequence of the peaks of sediment and discharge, all three types of flood produce anti-clockwise hysteresis loops, implying a non-limited sediment supply environment in the flood season and the intensive sediment carrying capability of hyperconcentrated flow. Concerning the variability of sediment transport at monthly and seasonal scales, different from those of the within-flood scale, almost all the hysteresis loops are clockwise loops. Sediment transport mainly concentrates on summer and early autumn, while seasons of winter, spring and late autumn are in preparation for discharge of sediment, giving a 'store–release' cycling process on a seasonal scale. Annually, the *C* values vary from 77 to 605 kg m^{-3}, giving a mean annual value of approximately 305 kg m^{-3}, and the total suspended sediment transported during the 1960–1967 period was estimated at 3055×10^4 tonnes, with a specific sediment yield $2{\cdot}042 \times 10^4$ t km^{-2} $year^{-1}$, which has a large variability, ranging from the minimum value of 39×10^4 tonnes in 1965 to the largest, 1326×10^4 tonnes, in 1966, with 1·05 coefficient of variation. The high degree of variability in suspended load and *C* values can be primarily related to the number and magnitude of the floods.

Acknowledgements

The authors wish to acknowledge the projects of the National Grand Fundamental Research 973 Program of China under Grant No. 2007CB407207 and the National Natural Science Foundation of China under Grant No. 30671721 for their financial support of this work. Special thanks are owed to two anonymous reviewers and Professor Kirkby for their fruitful suggestions to the improvement of the manuscript.

References

Alexandrov Y, Laronne JB, Reid I. 2003. *Suspended Sediment Transport in Flash Floods of the Semiarid Northern Negev, Israel*. IAHS Publication 278; 346–352.

Alexandrov Y, Laronne JB, Reid I. 2007. Intra-event and inter-seasonal behaviour of suspended sediment in flash floods of the semi-arid northern Negev, Israel. *Geomorphology* **85**: 85–97.

Asselman NEM. 1999. Suspended sediment dynamics in a large drainage basin: the River Rhine. *Hydrological Processes* **13**: 1437–1450.

Cai QG, Luk SH, Li G, Ma S. 1992. Calculation of sediment delivery ratio and sediment delivery law in Yangdaogou basin. In *Soil Erosion Management and Application of Geographical Information System in the Loess Plateau Region, Western Shanxi*, Wang F (ed.). Sciences Press: Beijing; 113–127.

Chen SL, Zhang GA, Yang SL, Shi JZ. 2006. Temporal variations of fine suspended sediment concentration in the Changjiang River estuary and adjacent coastal waters, China. *Journal of Hydrology* **331**: 137–145.

Chen YZ. 1983. A preliminary analysis of the processes of sediment yield in small catchment on the Loess Plateau. *Geographical Research* **2**: 35–47.

Collins AD, Walling DE, Leeks GJL. 1997. Fingerprinting the origin of fluvial suspended sediment in large river basins: combining assessment of spatial provenance and source type. *Geografiska Annaler* **79A**: 239–254.

de Boer DH, Campbell IA. 1989. Spatial scale dependence of sediment dynamics in a semi-arid badland drainage basin. *Catena* **16**: 277–229.

Dieckmann H, Motzer J, Seuffert O, Harres HP. 1989. Vegetation vs. erosion. The example of the Pixinamanna Catchment in southern Sardinia. *Geoöko* **2**: 11–24.

Ferguson RI. 1986. River loads underestimated by rating curves. *Water Resource Research* **21**: 74–76.

Gardner LR, Kjerfve B. 2006. Tidal fluxes of nutrients and suspended sediments at the North InleteWinyah Bay National Estuarine Research Reserve. *Estuarine, Coastal and Shelf Science* **70**: 682–692.

Gomez B, Phillips JD, Magilligan FJ, James LA. 1997. Floodplain sedimentation and sensitivity: summer 1993 flood, upper Mississippi River valley. *Earth Surface Processes and Landforms* **22**: 923–936.

Gong SY. 1988. Particular features of soil erosion on the Loess Plateau of the Yellow River Gully. *Soil and Water Conservation in China* **9**: 1–9.

Gong SY, Jiang DL. 1978. Soil and water loss and prevention in loess hilly region on the Loess Plateau in middle reaches of Yellow River. *Sciences in China: D Series* **6**: 671–678.

Gong SY, Xiong GS. 1980. The origin and transport of sediment of the Yellow River. In *Proceedings of 1st International Conference on River Sediment*. Guanghua: Beijing; 43–50.

Haifa MK. 1984. Anti clockwise hysteresis for suspended sediment concentration during individual storms: Holbeck Catchment; Yorkshire, England. *Catena* **11**: 251–257.

Heidel SG. 1956. The progressive lag of sediment concentration with flood waves. *Transaction American Geophysical Union* **37**: 56–66.

Horowitz AJ, Elrick KA, Smith J. 2001. Estimating suspended sediment and trace element fluxes in large river basins: methodological considerations as applied to the NASQAN programme. *Hydrological Processes* **15**: 1107–1132.

Hudson PF. 2003. Event sequence and sediment exhaustion in the lower Panuco Basin, México. *Catena* **52**: 57–76.

Jing K, Chen Y, Li F. 1993. *Sediment and Environment of Yellow River*. Science: Beijing.

Kimura R, Liu Y, Takayama N, Zhang X, Kamichika M, Matsuoka N. 2005. Heat and water balances of the bare soil surface and the potential distribution of vegetation in the Loess Plateau, China. *Journal of Arid Environment* **63**: 439–457.

Lavigne F, Suwa H. 2004. Contrasts between debris flows, hyperconcentrated flows and stream flows at a channel of Mount Semeru, East Java, Indonesia. *Geomorphology* **61**: 41–58.

Lenzi MA, Marchi L. 2000. Suspended sediment load during floods in a small stream of the Dolomites (northern Italy). *Catena* **39**: 267–282.

Lirer L, Vinci A, Alberico I, Gifuni T, Bellucci F, Petrosino P, Tinterri R. 2001. Occurrence of inter-eruption debris flow and hyperconcentrated flood-flow deposits on Vesuvio volcano, Italy. *Sedimentary Geology* **139**: 151–167.

Liu JG, Cai QG, Liu QJ, Li YY. 2005. Study on the regularity of sediment yield processes in catchments under different scales. *Journal of Sediment Research* **4**: 7–13.

Magilligan FJ, Phillips JD, James AJ, Gomez B. 1998. Geomorphic and sedimentological controls on the effectiveness of an extreme flood. *Journal of Geology* **106**: 87–95.

Ministry of Water Conservancy and Electric Power PRC. 1962. *National Standards for Hydrological Survey*, Vols 1–7. China Industry Press: Beijing.

Ministry of Water Conservancy and Electric Power PRC. 1975. *Handbook for Hydrological Survey*, Vols 1–3. Water Conservancy and Electric Power Press: Beijing.

Mossa J. 1988. Discharge-sediment dynamics of the lower Mississippi River. *Transactions Gulf Coast Association of Geological Societies* **38**: 303–314.

Mou J, Meng Q. 1982. On the sediment delivery ratio for calculating sediment yield. *Journal of Sediment Research* **2**: 60–65.

Novotny V, Chesters G. 1989. Delivery of sediments and pollutants from nonpoint sources: a water quality perspective. *Journal of Soil Water Conservation* **44**: 568–576.

Rondeau B, Cossa D, Gagnon P, Bilodeau L. 2000. Budget and sources of suspended sediment transported in the St. Lawrence River, Canada. *Hydrological Processes* **1**4: 21–3.

Rovira A, Batalla JR. 2006. Temporal distribution of suspended sediment transport in a Mediterranean basin: the Lower Tordera (NE SPAIN). *Geomorphology* **79**: 58–71.

Shi H, Shao MA. 2000. Soil and water loss from the Loess Plateau. *Journal of Arid Environments* **45**: 9–20.

Siakeu J, Oguchi T, Aoki T, Esaki Y, Jarvie HP. 2004. Change in riverine suspended sediment concentration in central Japan in response to late 20th century human activities. *Catena* **55**: 231–254.

Sichingabula HM. 1998. Factors controlling variations in suspended sediment concentration for single-valued sediment rating curves, Fraser River, British Columbia, Canada. *Hydrological Processes* **13**: 1035–1050.

Spott D, Guhr H. 1994. The dynamics of suspended solids in the tidally unaffected River Elbe as a function of flow and shipping.

Steegen A, Govers G. 2001. Correction factors for estimating suspended sediment export from loess catchments. *Earth Surface Processes and Landforms* **26**: 441–449.

Steegen A, Govers G, Takken I, Nachtergaele J, Merckx R. 2001. Factors controlling sediment and phosphorus export from two Belgian agricultural catchments. *Journal of Environmental Quality* **30**: 1249–1258.

Svendsen J, Stollhofen H, Krapf CBE, Stanistreet IG. 2003. Mass and hyperconcentrated flow deposits record dune damming and catastrophic breakthrough of ephemeral rivers, Skeleton Coast Erg, Namibia. *Sedimentary Geology* **160**: 7–30.

Tang KL. 1991. *Soil Erosion on the Loess Plateau: its Regional Distribution and Control*. China Science and Technology: Beijing; 246.

Tang KL, Zhang KL, Lei A. 1998. Critical slope gradient for compulsory abandonment of farmland on the hilly Loess Plateau. *Chinese Science Bulletin* **4**3: 409–412.

Walling DE, Owens PN, Leeks GJL. 1999. Fingerprinting suspended sediment sources in the catchment of the River Ouse, Yorkshire, UK. *Hydrological Processes* **13**: 955–975.

Walling DE, Peart MR, Oldfield F, Thompson R. 1979. Suspended sediment sources identified by magnetic measurements. *Nature* **281**: 110–113.

Walling DE, Webb BW. 1982. Sediment availability and the prediction of storm-period sediment yields. In *Recent Developments in the Explanation and Prediction of Erosion and Sediment Yield*. IAHS Publication 137; 327–337.

Wan Z, Shen S. 1978. Hyperconcentrated flow in the Yellow River in relation to its channel forming. In *Selected Research Reports on Sedimentation of the Yellow River*. Research Group of Yellow River Sedimentation.

Wang XL, Qiang N, Hu WD. 1982. The formation and processes of confluence of the hyperconcentrated flow in the gullied-hilly loess areas of the Yellow River basin. *Shuili Xuebao* **7**: 26–35.

Williams GP. 1989. Sediment concentration versus water discharge during single hydrologic events in rivers. *Journal of Hydrology* **111**: 89–106.

DOI: 10.1002/esp

Wood PA. 1977. Controls of variation in suspended sediment concentration in the River Rother, West Sussex, England. *Sedimentology* **24**: 437–445.
Xia J, Qiao YF, Song XF, Ye AZ, Zhang XC. 2007. Analysis about effect rules of underlying surface change to the relationship between rainfall and runoff in the Chabagou Catchment. *Resources Science* **29**: 70–76.
Xu JX. 1991. Erosion caused by hyperconcentrated flow on the Loess Plateau of China. *Catena* **36**: 1–19.
Xu JX. 1999. Grain-size characteristics of suspended sediment in the Yellow River, China. *Catena* **38**: 243–263.
Xu JX. 2004. Hyperconcentrated flows in the slope-channel systems in gullied hilly areas on the Loess Plateau, China. *Geografiska Annaler* **86A**: 349–366.
Yan Y. 1984. *An Introduction to Hydrometry*. Water Conservancy and Electric Power Press: Beijing.

DOI: 10.1002/esp